Single Stage Power Control Strategy for Nanogrid Connected Solar PV System

Rakesh Namani[1,*], Babu Natarajan[2], Senthilkumar Subramaniam[2] and Madhusudanan Gurusamy[3]

[1]*Department of EE, Rajiv Gandhi University of Knowledge Technologies, Basar, Telangana, India*
[2]*Department of EEE, National Institute of Technology, Tiruchirappalli, Tamilnadu, India*
[3]*Department of EEE,SRM Valliammai Engineering College, Chengalpattu, Tamilnadu, India*
E-mail: namanirakesh@rgukt.ac.in
[*]*Corresponding Author*

Received 08 June 2021; Accepted 01 December 2021;
Publication 16 February 2022

Abstract

The focus on reduction of converter size in nanogrid connected Photo-Voltaic (PV) systems increases to obtain the various advantages. This paper proposes a single stage nanogrid connected solar PV system that works with DC-AC inverter along with the closed loop control strategy to send the maximum power from the PV array. The proposed scheme controls the power delivery of the PV system to nanogrid in a single stage power conversion along with the incorporated Maximum Power Point Tracking (MPPT) controller. The decoupled control strategy has been designed and developed for the proposed system using synchronous reference frame theory. The developed hardware prototype in the laboratory has been used to validate MATLAB/Simulink simulation results. The simulation and experimental results have been observed

Distributed Generation & Alternative Energy Journal, Vol. 37_3, 749–770.
doi: 10.13052/dgaej2156-3306.37317

for dynamic changes in irradiation by maintaining the Total Harmonic Distortion (THD) within the standard limits while operating at unity power factor. The successful validation of the proposed control strategy shows its usefulness in real-time nanogrid applications.

Keywords: Single stage power conversion, nanogrid, decoupled control strategy, maximum power point tracking, and DC-AC inverter.

1 Introduction

The increased demand of electrical energy, increased prices of fossil fuels such as petroleum, coal, natural gas, heavy crude oil etc. makes us to use Renewable Energy Sources (RES). Among the available RES, solar energy has the benefits of inexhaustible, clean and environment friendly [1]. Now a day, the advanced power electronic controllers are used to harness maximum power output and which has less operational and maintenance costs. As many of the electrical loads are operated with AC power supply, AC transmission is preferred over DC transmission. Therefore, DC power produced in solar PV systems are converted into suitable AC power supply and fed to utility grid. To regulate the terminal voltage, constant frequency and also for feeding electrical power to utility grid it requires suitable power electronic controllers [2].

A grid-connected solar PV system has become most popular application of solar energy [3]. MPPT technique is applied in grid-connected photovoltaic system to enhance the power fed to grid [4]. Solar PV system, which uses a multi-level inverter for feeding power is little complex in developing its control algorithm [5]. Modelling of Grid-connected PV system control strategy with three phase three level inverter is examined [6]. The capacitor voltage balance limit is a major constraint in a multilevel converter based energy storage system as discussed in [7]. Hence, multi-level inverter with space-vector PWM method is implemented [8]. The variation of middle point voltage control for three level VSI is implemented with modified PWM control scheme [9]. Further, the three level voltage source inverters are implemented with randomized voltage vector switching scheme [10]. The single stage three phase solar PV system has improved maximum power tracking capability [11]. The single stage grid-connected solar PV systems have benefits such as simple structure, high efficacy, etc. Now a day, grid-connected solar PV system becomes more popular in most of the applications [12, 13]. However, the control objectives such as the synchronization with the utility

voltage, peak power point tracking and reduction of harmonics in grid current need to be considered [14]. Various peak power point tacking techniques are implemented for uniform insolation and non-uniform insolation on PV array to extract global peak power from PV modules [15]. The most popular and widely used MPPT method for PV modules is Perturb & Observe (P&O), because of its less complexity. By using conventional series–parallel connection, various topologies are proposed to link local PV generation system to grid [16].

Now a day, single stage grid-connected solar PV systems becomes more popular as it does not require any storage systems such as batteries and also the capital cost is reduced [17]. The extraction of maximum power from PV modules becomes essential because of its high initial cost and less span of life. There are mainly two types of power electronic configurations in grid-connected PV systems such as single stage and two stage power conversions between PV array and grid. In two stage configuration of a grid connected solar PV system, DC-DC converter succeeded by DC-AC inverter [18, 19] as given in Figure 1(a). The DC-DC converter is used to get the variable resistance across the PV array terminals and also to give the required DC voltage at input of DC-AC inverter stage. The power transferred to the grid is achieved by generating the sinusoidal voltages and currents from the inverter. It has lower reliability, larger filter size and less efficiency. The harmonics reduction is achieved by implementing a modified Sinusoidal Pulse Width Modulation (SPWM) based switching strategy [20]. Further, nano-grids with the renewable energy sources are complex systems and also depend on

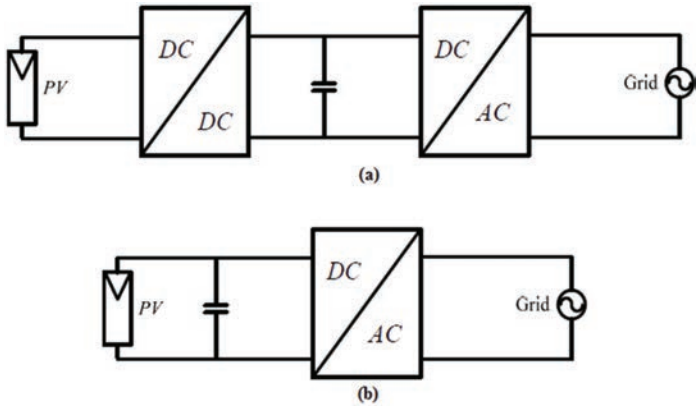

Figure 1 Grid-connected converter configuration (a) Conventional two-stage nanogrid configuration (b) Single-stage nanogrid configuration.

different dynamic sources to feed various applications. The International Renewable Energy Agency (IRENA) report highlights about nano-grid such as improving the resilience and reliability in power system by integrating the wind and solar power generation sources. The renewable nano-grids are different from the main grid, because the islands and remote areas can also get the reliable electricity from renewable nano-grids [21].

This paper elaborates the single stage grid connected solar PV system and its control technique. The single stage power converters block diagram is as shown in Figure 1(b). The objectives of two stage power converters need to be fulfilled by single stage power converter. Single stage conversion can be achieved by two methods with low cost and higher efficiency. One of the methods is cascaded inverter with step-up transformer, and the other is PV array with sufficiently large voltage. The large voltage at PV array suffers due to partial shading of the PV modules. Among the two methods, inverter followed by the transformer configuration is most commonly used for the single stage power conversion. DC-AC voltage source inverters have been widely used in industry for single stage DC to AC power conversion.

After detailed literature survey, the problems identified are as follows: (i) two stage power conversion, (ii) less power delivery between PV array and grid, (iii) dedicated power converter for MPPT. Hence, the objectives of the proposed method to address afore mentioned problems are as follows: (i) Developing the single stage power converter, (ii) Design of controller for maximum power delivery between solar PV array and grid, (iii) Incorporating MPPT in single stage converter.

This paper organized as follows: The proposed single stage grid connected solar PV system is discussed in Section 2. The results and discussions are elaborated in Section 3. Finally, Section 4 is given with the conclusions remarks.

2 Proposed Single Stage Grid Connected Solar PV System

The proposed nanogrid connected PV system is given in Figure 2. It consists of the solar PV array at its input terminal, MPPT controller to obtain maximum power, DC-AC inverter to integrate solar PV array with the nanogrid, transformer matches the inverter output voltage with voltage of the nanogrid, a small size inductive filter to minimize nanogrid current harmonics, and DC link capacitor to reduce DC link voltage ripples. The decoupled current control strategy is used to control the power flow between the PV array and nanogrid.

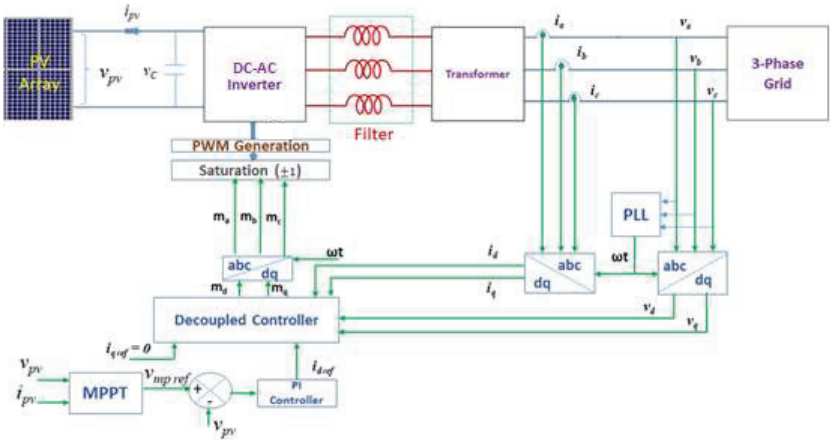

Figure 2 Block diagram for proposed nanogrid configuration.

Further, DC-AC Inverter is connected to PV array through suitable DC link capacitor. The output of PV array voltage is maintained constant by using MPPT controller. The closed loop control strategy for DC-AC Inverter is used to feed the power to the nanogrid. It is known that the obtained power from the solar PV array varies widely and it is directly fed to the nanogrid. The flowchart for the proposed control strategy is given in Figure 3.

The voltage controller is used to generate the reference for the control of active power. It compares the voltage at DC bus and the generated reference voltage by MPPT controller by following the Proportional Integral (PI) controller. The PI controller's output provides the active current component (i_{dref}) and reactive power control achieved with the reactive current component. Depending on the reactive power requirement to the nanogrid, the component of reactive current is adjusted. If nanogrid is not demanding for reactive power then the component of reactive current is adjusted to zero.

The inverter output voltage is the vector sum of voltages at AC grid and the series drop of across the filter. The voltage equation for three phases is given below:

$$v_a = V_{ga} + Ri_a + L\frac{di_a}{dt} \tag{1}$$

$$v_b = V_{gb} + Ri_b + L\frac{di_b}{dt} \tag{2}$$

$$v_c = V_{gc} + Ri_c + L\frac{di_c}{dt} \tag{3}$$

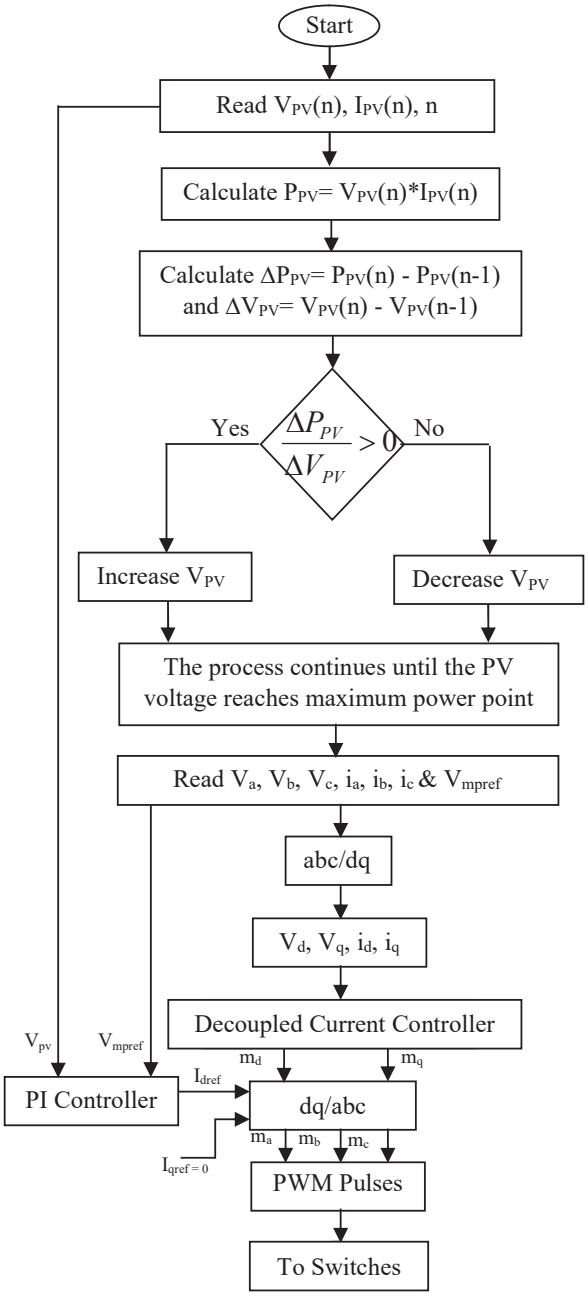

Figure 3 Flowchart for the proposed control strategy.

where, V_{ga}, V_{gb}, and V_{gc} are the nanogrid voltages. V_a, V_b, and V_c are the output voltages at inverter. The total inductance between the nanogrid and inverter is L. R is the resistance of filter.

The above equations are altered into *dq* quantities by using synchronously rotating *dq* reference frame. The modified equations are;

$$v_d = V_{gd} + Ri_d + L\frac{di_d}{dt} - \omega L i_q \tag{4}$$

$$v_q = V_{gq} + Ri_q + L\frac{di_q}{dt} - \omega L i_d \tag{5}$$

Where, V_{gd} and V_{gq} are the AC system voltage components, i_d and i_q are the AC system current components and v_d and v_q are inverter output voltages in the *dq*-frame.

The relationship between v_d and m is given as:

$$v_d = m_d\frac{v_{dc}}{2} \tag{6}$$

$$v_q = m_q\frac{v_{dc}}{2} \tag{7}$$

The true and reactive power delivered to the AC side is,

$$p = \frac{3}{2}(V_{gd}i_d + V_{gq}i_q) \tag{8}$$

$$q = \frac{3}{2}(-V_{gd}i_q + V_{gq}i_d) \tag{9}$$

Under steady state and nanogrid synchronized condition, $V_{gq} = 0$. The above equations can be written as,

$$p = \frac{3}{2}V_{gd}i_d \tag{10}$$

$$q = \frac{-3}{2}V_{gd}i_q \tag{11}$$

Therefore, based on Equations (10) and (11), *p* and *q* are controller by i_d and i_q respectively.

$$i_{dref} = \frac{2}{3V_{gd}}p_{ref} \tag{12}$$

$$i_{qref} = \frac{2}{3V_{gd}}q_{ref} \tag{13}$$

From the above equations, if $i_d \approx i_{dref}$ and $i_q \approx i_{qref}$, then the injection of desired reactive power and true power into the nanogrid. The fast tracking of reference is achieved using the voltage and current controllers. From these, it can say that *p* and *q* are independently controlled by their respective reference commands.

In Equations (4) and (5), i_d and i_q are state variables, v_d and v_q are control inputs, and V_{gd} and V_{gq} are disturbance inputs. Due to the presence of $L\omega_0$ terms in Equations (4) and (5), the dynamics of i_d and i_q are coupled. To decouple, dynamics of m_d and m_q are determined as follows

$$m_d = \frac{2}{v_{dc}}(u_d + V_{gd} - \omega L i_q) \tag{14}$$

$$m_q = \frac{2}{v_{dc}}(u_q + V_{gq} - \omega L i_d) \tag{15}$$

Where u_d and u_q are two new control inputs. Whereas,

$$L\frac{di_d}{dt} = u_d - Ri_d \tag{16}$$

$$L\frac{di_d}{dt} = u_q - Ri_q \tag{17}$$

The above equations describe two decoupled first-order linear systems. Based on Equations (16) and (17), i_d and i_q can be controlled by u_d and u_q respectively. Figure 4 shows a block diagrammatic representation of the $d-q$ axis current controllers of the solar PV system connected to nanogrid in which u_d and u_q are the outputs of two corresponding compensators. The error $e_d = i_d^{ref} - i_d$ processed from d-axis compensator and provides u_d. Then, based on Equation (14), u_d contributes to m_d. Similarly, the error $e_q = i_q^{ref} - i_q$ processed from q-axis compensator and provides u_q. Then based on Equation (15), u_q contributes to m_q. The voltage source inverter amplifies m_d and m_q by a factor of $\frac{v_{dc}}{2}$ and generates V_d and V_q that in turn control i_d and i_q. As all signals are DC quantities, a simple PI compensator is sufficient to enable tracking of DC reference commands. These two PI regulators compensate any existing error by generating appropriate control voltages u_d and u_q, which are altered back to phase quantities (m_a, m_b, m_c) and are given as inputs to PWM block to generate the command signals to the switches of inverter.

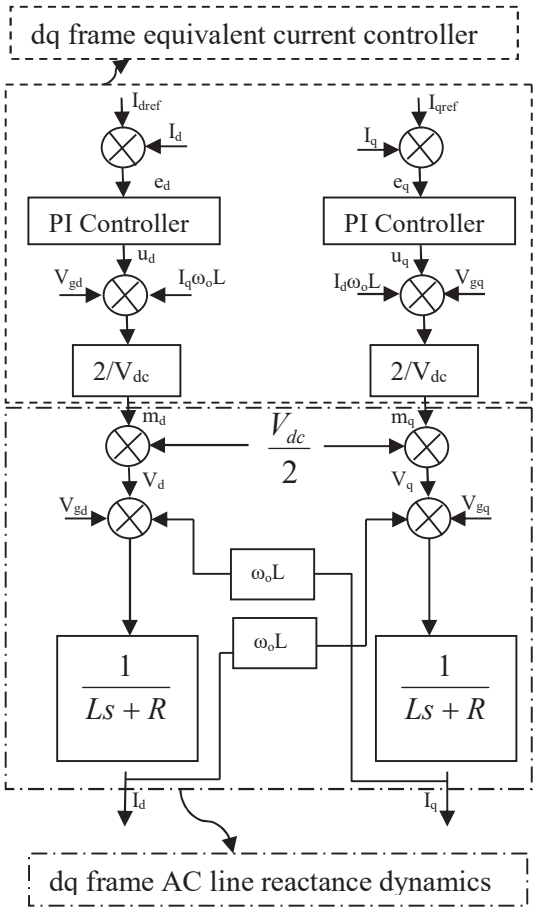

Figure 4 Control block diagram of a current controlled voltage source inverter.

3 Results and Discussion

The MATLAB/Simulink simulated and hardware results of the single stage nanogrid connected solar PV system with proposed controller using dSPACE 1103 controller board are presented. The proposed system performance obtained through simulation are validated with the experimentally developed 500 W prototype consist of three PV modules connected in series with each module rating of 166.6 W. The PV array is designed based on the module parameter values presented in Table 1. The complete experimental set up is shown Figure 5. It consists of DC-AC inverter along with the gate drive circuit

Table 1 Specifications of PV module

Parameter	Value
PV module power, P_o	166.8 W
PV module open circuit voltage, V_{oc}	46 V
PV module short circuit current, I_{sc}	4.7 A
Maximum module voltage, V_{mp}	37.5 V
Maximum module current, I_{mp}	4.45 A
Number of modules in series	3

Table 2 Specifications of DC-AC inverter

Parameter	Value
Inverter DC voltage	0–600 V DC
Output AC voltage	415 V AC
Output current	30 A max
Switching frequency	20 kHz max
Ambient temperature	45°C
Cooling method	Forced air cooled

Table 3 Specifications of LEM voltage sensor LV 25-P

Parameter	Value
Primary involved potential, V_{PN}	DC/AC 500 V
Supply voltage, V_c	12 V to 15 V DC
Primary nominal RMS current, I_{PN}	0 to 10 mA
Conversion ratio, K_N	2500:1000
Secondary nominal RMS current, I_{SN}	25 mA

Table 4 Specifications of LEM current sensor LA 55-P

Parameter	Value
Primary nominal RMS current, I_{PN}	50 A DC/AC
Conversion ratio, K_N	1:1000
Secondary nominal RMS current, I_{SN}	50 mA

with the specifications as given in Table 2 along with the autotransformer to set the nanogrid voltage to 62V and L-filter. For sensing the currents and voltages, LEM based voltage and current sensors are used with the specifications as given in Tables 3 and 4. The proposed controller performance is observed by implementing in dSPACE 1103 real time controller software desk. For modelling and code generation MATLAB/Simulink Real-Time Workshop by the Math Works and the Real-Time Interface by dSPACE are installed. Control desk software from dSPACE is used as a front end and serves to

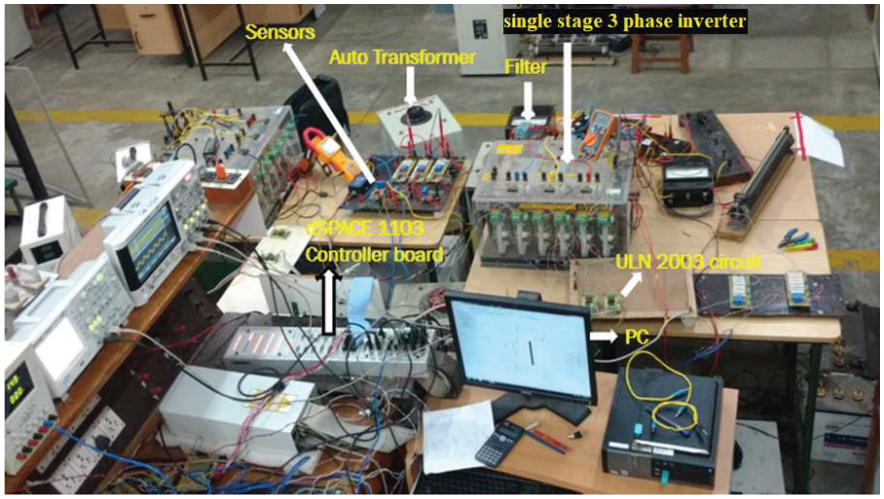

Figure 5 Experimental set-up of single stage nanogrid connected solar PV system.

Figure 6 dSPACE 1103 controlled board.

provide instrumentation, parameterization, measurements, and experiment control as shown in Figure 6. The three phase nanogrid parameters are line to line voltage of 62.46 V and frequency of 50 Hz. The simulation results obtained for 1000 W/m^2 is from 1 to 1.5 s and 700 W/m^2 is from 1.5 to 2 s. The experimental results are obtained for 1000 W/m^2 is from $t = 0$ to t_1 sec and 700 W/m^2 is from $t > t_1$ sec. The temperature is kept constant at 25°C.

PV systems equipment such as step-up transformers and electrical cables are not sources of electromagnetic interference because of their low-frequency (50 Hz) of operation and PV panels themselves do not emit EMI.

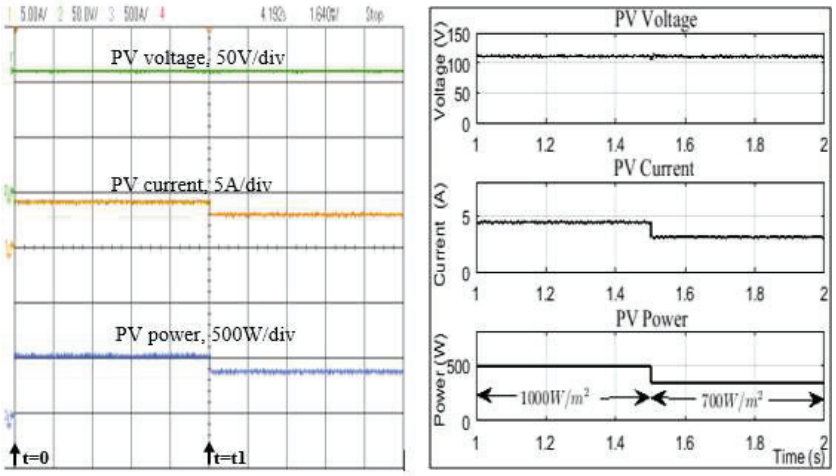

Experimental Simulation

Figure 7 Dynamic response of PV parameters for step change in irradiance from 1000 W/m^2 to 700 W/m^2.

The only component of a PV array that may be capable of emitting EMI is the inverter. Hence, synthesizing a stepped output voltage allows reduction in harmonic content of voltage waveform. This results in increasing the quality of output waveform and reducing the size and cost of the output filter. The staircase output voltage can improve the quality of the output voltage and reduce the voltage stress (dv/dt) on switching components. This can remedy the problem associated with Electro Magnetic Interference (EMI) problems.

The dynamic response of PV array parameters for step change in irradiance from 1000 W/m^2 to 700 W/m^2 is shown in Figure 7. A solar PV module with a maximum power of 166.6 W, maximum power voltage of 37.5 V, and maximum power current of 4.7 A is emulated in the 2 kW Chroma solar simulator 62020H-150S-Chroma-2014. Three such modules are connected in series and feed to the developed grid connected PV system. The required irradiations are adjusted as considered in the simulations results (700 W/m^2 and 1000 W/m^2) by using the solar simulator knobs. For irradiance of 1000 W/m^2: PV Voltage, PV Current and PV Power respectively are 112.5 V, 4.45 A and 500 W for simulation and experimentation. For irradiance of 700 W/m^2, the PV array voltage, PV current and PV power respectively are 111.8 V, 3.2 A and 358 W for simulation and 111 V, 3.2 A and 355 W for experimentation as shown in Figure 7. The grid phase voltage, current and power injected to nanogrid are shown in Figure 8. For irradiance

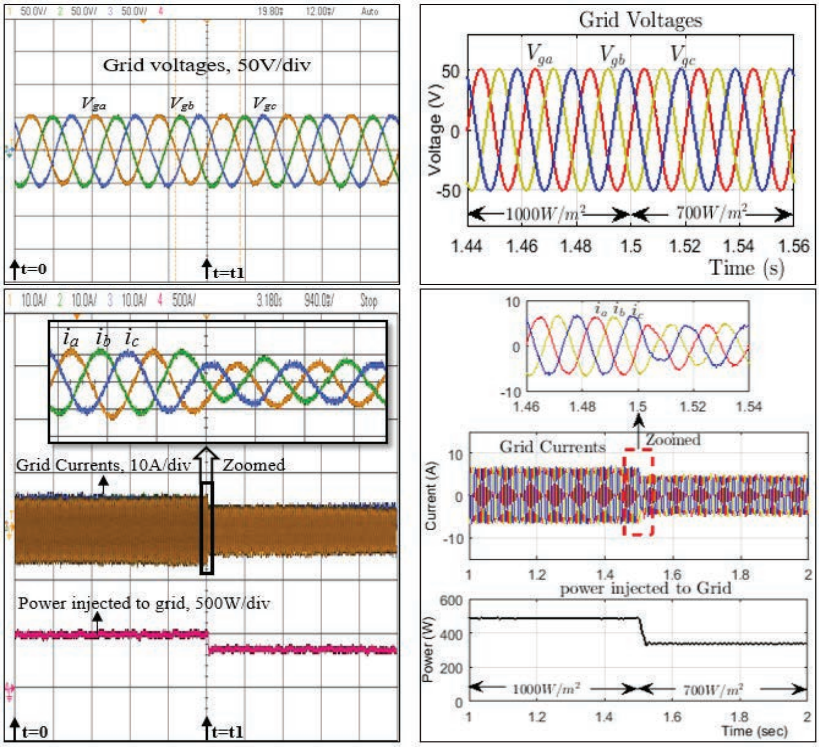

Experimental Simulation

Figure 8 Dynamic responses of grid side values for change in irradiance from 1000 W/m^2 to 700 W/m^2.

of 1000 W/m^2: grid phase voltage, current and power injected to nanogrid respectively are 36.06 V, 4.57 A and 495 W for simulation and 36.1 V, 4.06 A and 440 W for experimentation. For irradiance of 700 W/m^2: grid phase voltage (rms), current (rms) and power injected to nanogrid respectively are 36.06 V, 3.26 A and 353 W for simulation and 36.1 V, 2.88 A and 312 W for experimentation as shown in Figure 8.

Figure 9 shows the phase current and phase voltage in nanogrid. The phase current and phase voltage is almost in phase, which authenticates that the system is operating at unity power factor. Figure 10(a) shows the experimental result of the nanogrid current THD at 1000 W/m^2 and Figure 10(b) for THD at 700 W/m^2 respectively and the corresponding current THD value are 1.2% and 1.6% respectively. The simulation results for the nanogrid current THD at 1000 W/m^2 and 700 W/m^2 are given in Figure 10(c) and 10(d)

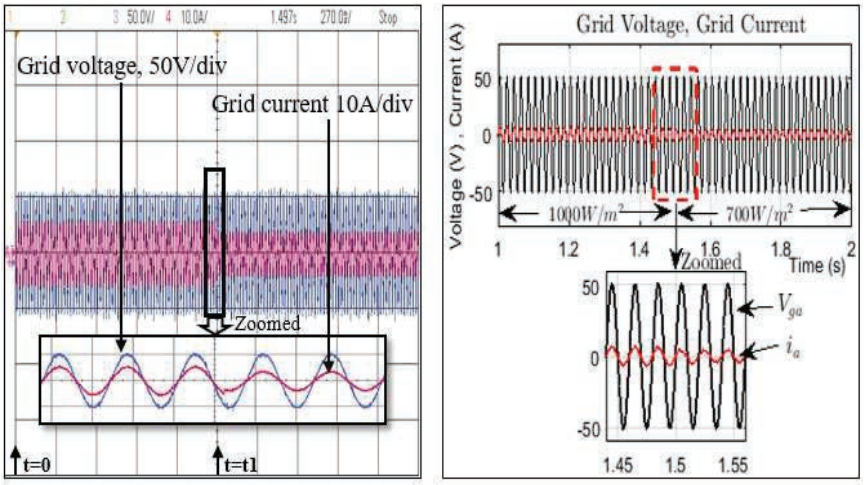

Experimental Simulation

Figure 9 Voltage and current waveforms of the nanogrid at unity power factor.

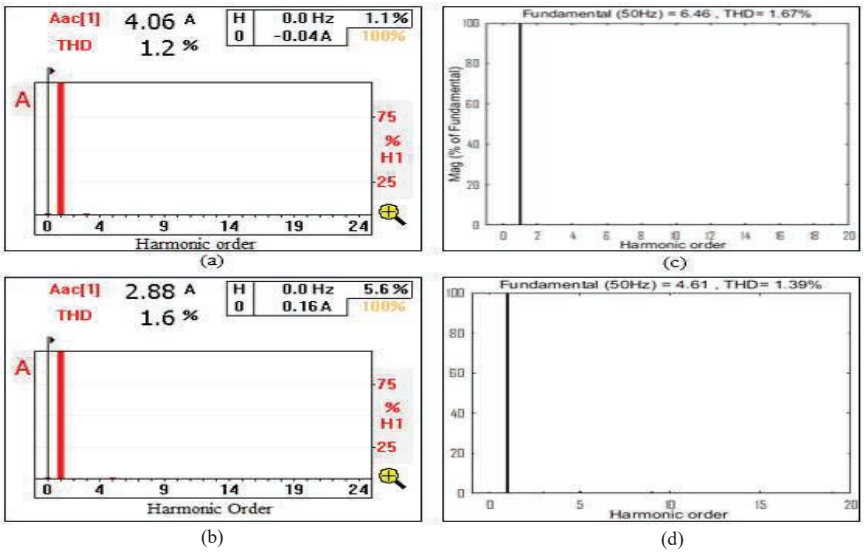

Experimental Simulation

Figure 10 Nanogrid current THD for step change in irradiance from 1000 W/m^2 to 700 W/m^2.

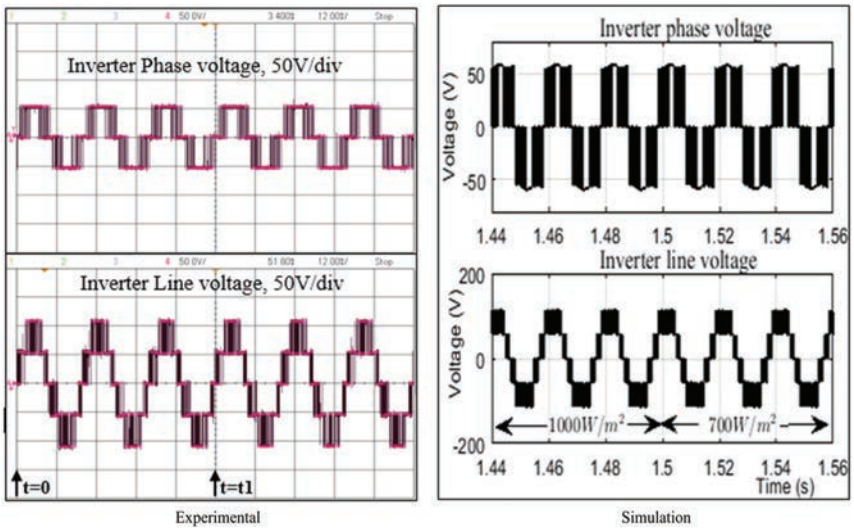

Figure 11 DC-AC inverter output voltages for step change in irradiance from 1000 W/m^2 to 700 W/m^2.

Table 5 Simulation and Experimental efficiency calculations with power loss analysis

Simulation	Experimentation
• **From t = 1 to 1.5 Sec (1000 W/m^2):**	• **From t = 0 to t$_1$ Sec (1000 W/m^2):**
DC: V = 112.5 V, I = 4.45 A, P = 500 W	DC: V = 112.5 V, I = 4.45 A, P = 500 W
AC: V_{ph} = 36.06 V, I = 4.57 A, P = 495 W	AC: V_{ph} = 36.1 V, I = 4.06 A, P = 440 W
Efficiency = 495/500 = 99%	Efficiency = 440/500 = 88%
• **Suddenly injecting the grid current:**	• **Suddenly injecting the grid current:**
At t = 1.5 Sec (700 W/m^2)	At t = t$_1$ Sec (700 W/m^2)
DC: V = 111.8 V, I = 3.2 A, P = 358 W	DC: V = 111.8 V, I = 3.2 A, P = 355 W
AC: V_{ph} = 36.06 V, I = 3.26 A, P = 353 W	AC: V_{ph} = 36.1 V, I = 2.88 A, P = 312 W
Efficiency = 353/358 = 98.6%	Efficiency = 312/355 = 87.8%

*In experimentation, the losses are due to the switching losses and I^2R drop.

respectively. The corresponding current THD values are 1.67% and 1.39% respectively. From above results, it is found that the values of current THD in nanogrid is well within the international standard (i.e., <5%). Figure 11 shows the DC-AC inverter output voltages for step change in irradiance from 1000 W/m^2 to 700 W/m^2. The simulation and experimental efficiency calculations with power loss analysis is given in Table 5. Further, the proposed control logic has been compared with the existed and highlighted the advantages as given in Table 6.

Table 6 Performance parameters comparison of proposed configuration with existed configurations

	Configurations		
Parameters	[12]	[13]	Proposed
Power level	Medium Power	HighPower	HighPower
Power Factor	0.98	Nearly Unity	Unity
Efficiency	NA	95%	99%
Inductor	1	4	3
Capacitor	1	3	1
Switch	4	4	6
Symmetrical/Unsymmetrical	Unsymmetrical	Unsymmetrical	Symmetrical
Frequency	20 KHz	4 KHz	5 KHz
Implementation of MPPT	P&O	Fuzzy	P&O
PV Module	BP-340	NA	Chroma solar simulator 62020H-150S
Grid Current THD	6.05%	$<5\%$	1.2%

4 Conclusion

This paper presented the control scheme for the single stage power conversion for nanogrid applications. The experimental results had been validated with simulation results for power delivery between solar PV array and nanogrid under different solar irradiance. The MPPT controller had been successfully incorporated in single stage converter with DC-AC inverter. Hence, the overall size of the converter was reduced. Decoupled control strategy was designed and developed for the proposed system using synchronous reference frame theory. The decoupled control strategy provides independent control over injection of true power to the nanogrid with the simultaneous tracking of the peak power from the PV array. The performance of the proposed scheme had been assessed through MATLAB/Simulink simulations and verified experimentally by means of dSPACE 1103 controller in laboratory. The successful validation of results shows the ability of the proposed control strategy to feed the peak PV power to the nanogrid. The values of current THD in nanogrid maintains very well within the range of IEEE-519 recommended standards while operating the system at unity power factor.

References

[1] Atika, Qazi., Fayaz, Hussain., Nasrudin, ABD, Rahim., Glenn, Hardaker., Daniyal, Alghazzawi., Khaleed, Haruna. Towards Sustainable

Energy: A Systematic Review of Renewable Energy Sources, Technologies, and Public Opinions, IEEE Access, 7, pp. 63837–63851, 2019, DOI: 10.1109/ACCESS.2019.2906402.

[2] Subramanian, Krithiga., N, AmmasaiGounden. Power electronic configuration for the operation of PV system in combined grid-connected and stand-alone modes. IET Power Electronics, 7, 3, pp. 640–647, 2014. DOI: 10.1049/iet-pel.2013.0107.

[3] Hamid, R, Teymour., Darmawan, Sutanto., Kashem, Muttaqi., Philip, Ciufo. Solar PV and battery storage integration using a new configuration of a three-level NPC inverter with advanced control strategy. IEEE Transactions on Energy Conversion, 29, 2, 354–365, 2014. DOI: 10.1109/TEC.2014.2309698.

[4] Elahe, Heydari., A, Y, Varjani. Combined modified P&O algorithm with improved direct power control method applied to single-stage three-phase grid-connected PV system. 9th Annual Power Electronics, Drives Systems and Technologies Conference (PEDSTC), 2018, pp. 347–351. DOI: 10.1109/PEDSTC.2018.8343821.

[5] A, M, Mahfuz-Ur-Rahman., Md, Rabiul, Islam., Kashem, M, Muttaqi., Dany, Sutanto. Model Predictive Control for a New Magnetic Linked Multilevel Inverter to Integrate Solar Photovoltaic Systems With the Power Grids.IEEE Transactions on Industrial Applications, 56, 6, 7145–7155, 2020. DOI: 10.1109/TIA.2020.3024352.

[6] Li, Zhang., Kai, Sun.,Yun, Wei., Xiaonan, Lu., Jinquan, Zhao. A Distributed power control of series connected module integrated inverters for PV Grid-tied applications. IEEE Transactions on Power Electronics, 33, 9, 7698–7707, 2018. DOI: 10.1109/TPEL.2017.2769487.

[7] Wei, Jiang., Chengwei, Zhu., Chen, Yang., Lei, Zhang., Shuai, Xue., Wu, Chen. The Active Power Control of Cascaded Multilevel Converter Based Hybrid Energy Storage System. IEEE Transactions on Power Electronics, 34, 8, pp. 8241–8253, 2019. DOI: 10.1109/TPEL.2018.2882450.

[8] Bheemaiah, Chikondra., Utkal, Ranjan, Muduli., Ranjankumar, Behera. Performance Comparison of Five-Phase Three-Level NPC to Five-Phase Two-Level VSI. IEEE Transactions on Industrial Applications, 56, 4, pp. 3767–3775, 2020. DOI: 10.1109/TIA.2020.2988014.

[9] Chen, Li., Tao, Yang., Ponggom, Kulsangcharoen., Giovanni, Lo, Calzo., Serhiy, Bozhko., C, Christopher, Gerada., P, Wheeler. A Modified Neutral Point Balancing Space Vector Modulation for Three-Level

Neutral Point Clamped Converters in High-Speed Drives. IEEE Transactions on Industrial Electronics, 66, 2, pp. 910–921, 2019. DOI: 10.1109/TIE.2018.2835372.

[10] Amritesh, Kumar., Vishal, Verma. Performance enhancement of single phase grid connected PV system under partial shading using cascaded multilevel converter. IEEE Transactions on Industrial Applications, 54, 3, 2665–2676, 2018. DOI: 10.1109/TIA.2017.2789238.

[11] Khalil, Alluhaybi., Issa, Batarseh., Haibing, Hu. Comprehensive review and comparison of single phase grid-tied photovoltaic micro-inverters. IEEE Journal of Emerging and Selected Topics in Power Electronics, 8, 2, pp. 1310–1329, 2020. DOI: 10.1109/JESTPE.2019.2900413.

[12] E, S, Sreeraj., K, Chatterjee., S, Bandyopadhyay. One-Cycle-Controlled Single-Stage Single-Phase Voltage-Sensorless Grid-Connected PV System. IEEE Transactions on Industrial Electronics, 60, 3, pp. 1216–1224, 2013. DOI: 10.1109/TIE.2012.2191755.

[13] Badar, N, Alajmi., Khaleed, H, Ahmed., Grain, Philip, Adam., Barry, W, Williams. Single-Phase Single-Stage Transformer less Grid-Connected PV System. IEEE Transaction on Power Electronics, 28, 6, pp. 2664–2676, 2013. 10.1109/TPEL.2012.2228280.

[14] A, Luna., Joan, Rocabert., Ignacio, Candela, J., J, Ramon, Hermoso. Grid Voltage Synchronization for Distributed Generation Systems Under Grid Fault Conditions. IEEE Transactions on Industry Applications, 51, 4, pp. 3414–3425, 2015, DOI: 10.1109/TIA.2015.2391436.

[15] Nishant,. Kumar., Bhim, Singh., Bijaya, Ketan, Panigrahi. Grid synchronisation framework for partially shaded solar PV-based microgrid using intelligent control strategy. IET Generation, Transmission & Distribution, 13, 6, pp. 829–837, 2018. DOI: 10.1049/iet-gtd.2018.6079.

[16] Bin, Guo., Yao, Sun., Hui, Wang., Bin, Liu., Xin, Zhang., Josep, Pou., Yongheng, Yang., Pooya, Davari. Optimization Design and Control of Single-Stage Single-Phase PV Inverters for MPPT Improvement. IEEE Transactions on Power Electronics, 35, 12, pp. 13000–13016, 2020. DOI: 10.1109/TPEL.2020.2990923.

[17] PrasanthKumar, Sahu., Madhav, D, Manjrekar. Controller Design and Implementation of Solar Panel Companion Inverters.IEEE Transactions on Industrial Applications, 56, 2, pp. 2001–2011, 2020. DOI: 10.1109/TIA.2020.2965867.

[18] Fan, Xie., Zhenxiong, Luo., Dongyuan, Qiu., Yanfeng, Chen., Liying, Huang. Study on a simplified structure of a two-stage grid-connected

photovoltaic system for parameter design optimization. Energies, 12, 2193, pp. 01–16, 2019. DOI: 10.3390/en12112193.

[19] Mitra, Mirhosseini., Josep, Pou., Vassilios, G, Agelidis. Single- and Two-Stage Inverter-Based Grid-Connected Photovoltaic Power Plants With Ride-Through Capability Under Grid Faults. IEEE Transactions on Sustainable Energy, 6, 3, pp. 1150–1159, 2015. DOI: 10.1109/TSTE .2014.2347044.

[20] Suhua, Luo., Fengjiang, Wu., Ke, Zhao. Modified Single-Carrier Multilevel SPWM and Online Efficiency Enhancement for Single-Phase Asymmetrical NPC Grid-Connected Inverter. IEEE Transactions on Industrial Informatics, 16, 5, pp. 3157–3167, 2020. DOI: 10.1109/TI I.2019.2906248.

[21] https://www.irena.org/publications/2020/Dec/Quality-infrastructure-for-smart-mini-grids.

Biographies

Rakesh Namani received his B.Tech degree in Electrical and Electronics Engineering from Kakatiya University, Warangal, Telangana, India, in 2008. He received his M.S (by Research) degree in Electrical and Electronics Engineering from the National Institute of Technology, Tiruchirappalli, Tamilnadu, India, in 2013. From June 2013 to February 2016, he served as an Assistant Professor with the Department of Electrical and Electronics Engineering, Kakatiya Institute of Technology and Science, Warangal, Telangana, India. From March 2016 to till date, he is working as an Assistant Professor with the Department of Electrical Engineering, Rajiv Gandhi University of Knowledge Technologies, Basar, Telangana, India. His research interests

include power electronics applications in renewable energy systems, grid-connected PV systems, and power enhancement of PV arrays.

Babu Natarajan received his M. Tech. degree in Embedded System technologies from Anna University, Tiruchirappalli, India. He is currently pursuing his Ph. D. degree at Nation Institute of Technology, Tiruchirappalli, India. His areas of interest include electrical drives, control and applications of power electronics in renewable energy systems.

Senthilkumar Subramaniam received the B.E. degree in Electrical and Electronics Engineering from Madurai Kamaraj University, Madurai, India, in 1999, the M.Tech. degree in Electrical Drives and Control from Pondicherry University, Puducherry, India, in 2005, and the Ph.D. degree in Electrical Engineering from the National Institute of Technology, Tiruchirappalli, India, in 2013. He has 20 years of teaching experience at various engineering institutions. He is currently working as an Associate Professor

with the National Institute of Technology. He has extensively researched on self-excited induction generators for standalone and grid-connected applications. His current research interests include the development of new power converter topologies for renewable energy systems and intelligent transportation systems.

Madhusudanan Gurusamy received his Bachelor's Degree in Electrical and Electronics Engineering from Bharathidasan University, Trichy, Tamil Nadu, India in the year 1997. He received his M.E. Degree in Power Electronics and Drives from Bharathidasan University, Tiruchirappalli during the year 2000. He received his Ph.D. degree in Electrical Engineering from National Institute of Technology, Tiruchirappalli in the year 2020. He has been working with the Department of Electrical Engineering, SRM Valliammai Engineering College, affiliated to Anna University, Chennai, India, since 2000. His research interests include Power Electronic Controllers for Renewable Energy System, Energy storage and Battery management system.